No Cage, No Tube: Relative Stabilities of Nanostructures

S. F. Li,[†,‡] Liming Gao,[‡] X. G. Gong,[§] and Z. X. Guo*[,†]

Department of Chemistry, University College London, London WC1H 0AJ, U.K.; School of Physics and Engineering, Zhengzhou University, Zhengzhou 450052, P. R. China; and Surface Physics Laboratory and Department of Physics, Fudan University, Shanghai 200433, P. R. China

Received: June 13, 2008

Relative stabilities of nanostructures are important in the design and selection of components for nanodevices. Here, we use first-principles simulations to evaluate the relative stabilities of representative nanostructures of semimetal Bi, semiconductive C, and metallic Au. The Bi_n cages are metastable and highly active and can readily transform to more stable three-dimensional amorphous structures upon activation. Both finite bismuth nanotubes and infinite nanotubes are even less stable than the cage structures. This is contrary to the cases for carbon, boron, and gold. The differences lie in their bonding characteristics and their responses to curvature. Our findings show tendencies of evolution of different types of nanostructures and also indicate that if a nanocage is (not) stable, then its nanotube is even more (less) stable. Hence, the stability of a cage structure predetermines the existence of a nanotube for a given element: i.e., no cage, no tube.

I. Introduction

Since the discovery of carbon fullerenes and nanotubes (CNTs),[1,2] stable cage- and tubelike structures have attracted considerable attention. Recently, simple graphene sheets have also been stabilized.[3] Other stable non-carbon cage structures, such as boron, boron nitride (semiconductive elements),[4,5] and Au_n (metal element),[6] have been identified both theoretically and experimentally. These structures are potential building blocks for nanodevices, such as novel one-dimensional conductors or wide-gap semiconductors, and carriers for clean energy and drug deliveries. It is interesting to note that nanotubes (NTs) are discovered for the elements that form nanocages (NCs).[7−9] From a topological point of view, these quasi-planar structures can be obtained by rolling up a closely packed atomic sheet, e.g., graphene, BN sheet, or the (111) plane of face-centered cubic (fcc) Au, into hollow cylinders or curved quasi-planar cages. Alternatively, these nanotubes can also be viewed as growing from a series of equatorial rings from a fullerene cage. This suggests that if an element with a quasi-layered structure can support a cagelike form, its NT may also be stable or vice versa. Understanding the relative stabilities of these nanostructures is important both in continued exploration of different types of nanostructures and in the design and assembly of the nanostructures into nanodevices.

Bismuth is the last element of group V, with a rhombohedral bulk configuration, which may be viewed as a quasi-layered structure where each atom has three nearest-neighbor atoms (3.07 Å).[10] It is also a semimetal favorable for electronic applications due to its highly anisotropic Fermi surface, small effective carrier masses, low carrier densities, and long carrier mean free path[10] compared with normal metals. Its unusual electronic properties present an attractive case for the study of quantum transport and finite size effects in nanostructures.[11] Recently, bismuth nanowires (BiNWs)[12] and nanotubes (BiNTs)[13] have been fabricated experimentally. Although bulk bismuth is a semimetal, bismuth nanostructures undergo a transition from a semimetal, with a small band overlap, to a semiconductor, with a small direct band gap, due to the quantum size effect.[11,12] However, the bismuth NTs are readily transformed into polycrystalline nanowires upon electron beam irradiations,[13] implying their metastability. Consequently, some interesting questions arise: (i) Why are BiNTs unstable? (ii) Are Bi_n cages (BiNCs) stable? (iii) What are the relative stabilities of NCs and NTs; e.g., can we prejudge the existence of an NT by predicting the stability of its NC? Answers to these questions, particularly the third one, may lead to a generalized criterion to assess the relative stabilities of nanostructures.

In this paper, we examined these questions using first-principles calculations by first investigating the stabilities of the bismuth cages, Bi_n ($n = 20, 32, 60$), and then comparing those with carbon, boron, and gold nanostructures. We identified that contrary to the semiconductive elements, carbon, boron, and metallic element gold, the semimetal bismuth does not form stable cagelike structures, which may be the basis of the instability of BiNTs observed experimentally.[13] We clarified that for a given element that can stabilize planar bonding or a two-dimensional (2D) nanostructure, its NTs are more stable than the NCs, which are more stable than the three-dimensional (3D) nanostructures. For an element that cannot form a stable NT, the stability sequence reverses.

II. Methods

Present calculations are based on the density functional theory (DFT)[14] with spin-polarized generalized gradient approximations (GGA),[15] as implemented in the VASP code.[16] The interaction of the valence electrons and the core is described with the projector-augmented wave (PAW) method,[17] including a scalar relativistic effect. The clusters are optimized in simple cubic supercells with the sizes of 20 and 30 Å for the small clusters (Bi_{20} and Bi_{32}) and the large Bi_{60}, respectively. For the cages, only Γ point was used for the Brillouin zone integrations. The total energy was converged to 0.001 eV for the structural relaxations. Ab-initio molecular dynamic (MD) simulations and the simulated annealing (SA) methods were also performed to

* To whom correspondence should be addressed.
† University College London.
‡ Zhengzhou University.
§ Fudan University.

10.1021/jp8052289 CCC: $40.75
Published on Web 08/05/2008

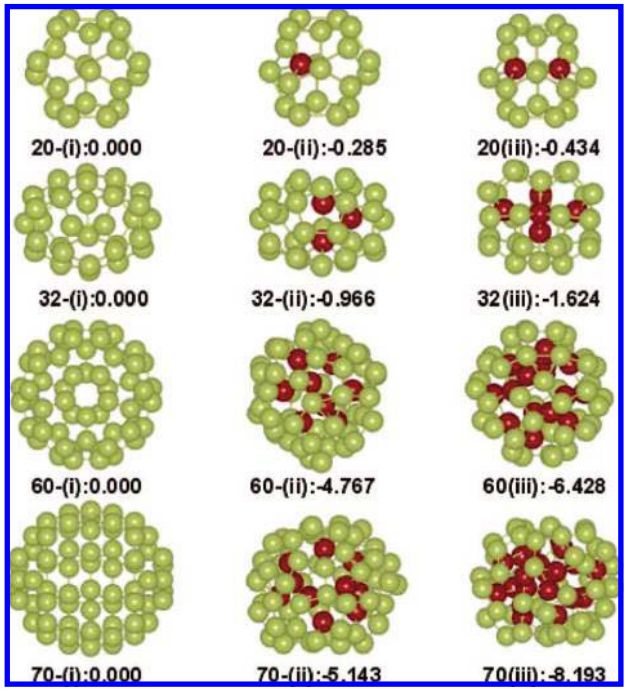

Figure 1. Low-lying geometric structures for Bi_n ($n = 20, 32, 60, 70$) clusters. The cage structures in the first column, n-i, are based on well-known fullerene structures and used as the energy references for the other two columns, where a more negative value (in eV) denotes a more stable structure. The red spheres denote the collapsed atoms from the surface.

generate random configurations and investigate the stability of these optimized structures. For the calculations of tubes, the Brillouin zones were sampled by $1 \times 1 \times 15$ special K-points using the Monkhorst scheme.[18] The current method and potential have been tested to be sufficiently accurate to describe the bismuth system, as reported previously.[19]

III. Results and Discussion

Cage structures of Bi_n ($n = 20, 32, 60$) with initial configurations similar to those of carbon fullerenes were optimized for each size (Figures 1(n-i)). The cages are well maintained with an average nearest bond length of 3.04, 3.05, and 3.06 Å and the HOMO−LUMO gaps of 0.46, 0.72, and 0.43 eV for I_h-Bi_{20}, D_{3h}-Bi_{32}, and I_h-Bi_{60}, respectively. Recently, we reported that the atoms of small Bi_n clusters ($n = 2-13$)[19] prefer to be three-coordinated and the Bi_{12} cluster favors a cage structure, which may be the basis of the existence of BiNTs. However, we find that the I_h-cage structure of Au_{32}[6] is about 6.168 eV less stable than the D_{3h} configuration, as in the Bi_{32} case. In such an I_h structure, there are only two different types of atomic sites on the cage: 12 five-coordinated sites and 20 six-coordinated sites, which may be the reason for its reduced stability compared with the 3-coordinated D_{3h}-Bi_{32} (Figure 1(32-i)). Surprisingly, we note that the average binding energies of these cages, defined as $E_b = -[E(Bi_n) - nE(Bi_{atom})]/n$, decrease as the cage size increases, from 1.996 (Bi_{20}), 1.968 (Bi_{32}) to 1.930 eV (Bi_{60}), contrary to the well-known general trend that the binding energy converges (increases) to the bulk value as cluster size increases. This implies that these cages are merely in metastable states.

The thermal stability of Bi_n cages are investigated by constant temperature MD simulations using the Nosé algorithm. In line with the average binding energy predications, the MD simulations confirm that a smaller Bi_n cage is more stable than a larger

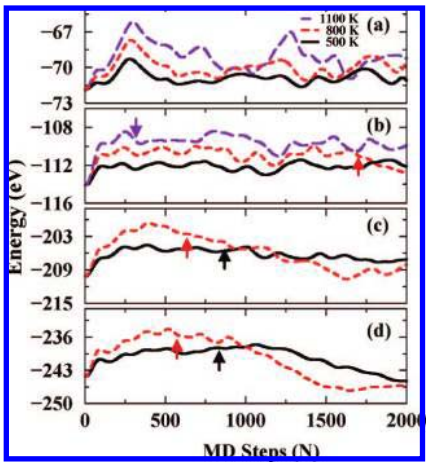

Figure 2. Total energy evolutions as a function of MD simulation steps for Bi_n ($n = 20, 32, 60, 70$) cages at different simulation temperatures. (a) $n = 20$, (b) $n = 32$, (c) $n = 60$, and (d) $n = 70$. The arrows indicate the thresholds of cage collapse.

one. The Bi_{20} structure, Figure 1(20-(i)), is almost intact after 2 ps of MD simulations at both 500 and 800 K, though the melting point of bismuth is 544.5 K. In fact, up to 1100 K, the Bi_{20} still possesses a fairly stable cage configuration within 2 ps MD simulation. This result implies its good thermal stability at low temperatures, as also indicated by the total free energy evolution in Figure 2a. On the other hand, the Bi_{32} cage, Figure 1(32-(i)), can only be maintained for 2 ps in the MD simulation at 500 K, and it starts to distort markedly after about 1.7 ps simulation at 800 K. The cage is hardly sustained for 0.4 ps at 1100 K, as shown in Figure 2b. Interestingly, different local structures of the Bi_{32} cage show different stabilities: the pentagons or hexagons in the relatively flat surface regions always tend to distort or break up prior to those with relatively large curvatures. For the Bi_{60} cage, a few atoms begin to collapse into the cage, after about 0.8 ps simulation at 500 K or 0.6 ps at 800 K. The total free energy begins to show evident decline, as marked by the arrows (Figure 2c). The results indicate that a smaller Bi cage is more stable than a larger one, from a thermostabilization point of view. In fact, we note from an MD simulation that the Bi_{12} cluster[19] can exist as an elongated cage for at least 4 ps at 1000 K.

The chemical stabilities of the Bi_n cages were further investigated by the adsorption of an additional Bi atom. In general, the more stable the structure, the more difficult for the additional atom to react with it. This is an important method of evaluating the chemical activity of structures both experimentally and theoretically. In each case, upon the adsorption of a single atom, the local structure at the adsorption site is considerably distorted after the adsorbed Bi atom binds with the three nearest-neighbor Bi atoms. The average bond length is about 3.11 Å, almost the same as in the Bi_n cages. One (two) Bi atom(s) is (are) evidently squashed into the Bi_{20} and Bi_{32} (Bi_{60} and Bi_{70}) cages, while most Bi atoms are still three-coordinated and the cage configurations are still well maintained. We note that the additional Bi atom favors the flat region of the Bi_{32} cage, indicating again the relatively high activity at these sites. The adsorption energies for the single Bi atom on Bi_n ($n = 20, 32, 60$) are 1.959, 2.058, and 2.512 eV, respectively, which are comparable with or larger than those of the cages. Hence, there must be new chemical bonds between the extra Bi atom and the large cages. For comparison, we also calculated the adsorption of one carbon atom on carbon fullerenes C_n. The C atom favors the bridge site with the fullerene structure almost

intact. The adsorption energies are 5.619, 4.107, and 3.670 eV, considerably smaller than the E_b (6.901, 7.287, and 7.664 eV) of C_n fullerences ($n = 20$, 32, and 60). It is also noted that the I_h-Au_{32} cage[6] can stably accommodate up to three inner Au atoms. The above results strongly indicate that the Bi_n cages are not stable.

To further evaluate the cage stability, a number of random 3D structures were generated for comparison. We note that many 3D structures of the same sizes are much more stable than the corresponding cages, particularly for the relatively large ones (Figure 1). For the Bi_{20} cage, the total energy is reduced by about 0.285 eV when one atom collapses into the cage, Figure 1(20-(ii)). The most stable structure of Bi_{20} accommodates two collapsed Bi atoms, leading to a 3D structure with C_{2h} symmetry, Figure 1(20-(iii)), which is about 0.434 eV lower in energy than the quasi-2D cage configuration, Figure 1(20-(i)). In this 3D-C_{2h} structure, the distance between the two collapsed Bi atoms is about 3.62 Å, slightly larger than the second-nearest neighbor distance of 3.53 Å in the bulk. For the Bi_{32} cluster, in Figures 1(32-(ii) and (iii)), two of the low-lying isomers are about 0.966 and 1.624 eV lower in energy than that of the cage, respectively. Five atoms collapsed in the most stable structure, Figure 1(32-(iii)). Similarly, the Bi_{60} cage is less stable than many 3D formless structures. The optimized 3D structure, Figure 1(60-(ii)), is 4.767 eV more stable than the cage, with about nine Bi atoms distributed inside the cluster. Figure 1(60-(iii)) shows the most stable structure with the maximum number (~14) of collapsed Bi atoms, resembling a core−shell configuration, which is 1.661 eV lower in energy than that in Figure 1(60-(ii)). It is interesting to note that the total energy of the cluster is lowered monotonously as the number of collapsed atoms increase. In these 3D structures, though perfect pentagons and hexagons are difficult to identify, most atoms still prefer to be three-coordinated. Although there is no guarantee that these are absolutely of the ground states, the stable 3D structures can unambiguously confirm that the Bi cage structures are unstable.

The instability of Bi_n ($n = 20$, 30, 60) cages may imply unstable single-walled Bi nanotubes (sWBiNTs). In fact, the Bi_{70} cage may be regarded as the shortest capped nanotube, as in the carbon case. It was found to be far less stable than many 3D amorphous structures, e.g., those shown in Figures 1(70-(ii)) and (70-(iii)), which are respectively 5.143 and 8.221 eV lower in energy than the tubelike structure, Figure 1(70-(i)). There are about 10 and 20 Bi atoms collapsed into the cage clusters, respectively, essentially destroying the cages. The collapse of the surface Bi atoms into the cluster was readily observed after 600−800 steps of MD simulations at 500 and 800 K, corresponding to the energy reduction in Figure 2d. These results support the experimental observation that metastable BiNTs readily transform to Bi polycrystalline nanowires upon electron beam irradiation.[13]

It is important to clarify why neither the BiNCs nor the SWBiNTs are stable, while carbon, boron, boron nitride, and gold can support both stable NCs and SWNTs. Considering the topology of the quasi-planar NCs and NTs, we calculated the average binding energies per atom (E_b) of (1) a monolayer (ML) hexagonal sheet, (2) the infinite armchair and zigzag NTs, and (3) the cages with sizes up to 70, for carbon, gold, and bismuth, as shown in Figures 3a−c, respectively. Here, the (3, 3), (4, 4), and (5, 5) armchair and the (5, 0), (6, 0), and (9, 0) zigzag NTs were selected, of which the pore diameters are close to those of the cages, respectively. For gold (Figure 3b), Au_n ($n = 7$, 10, 20, and 32) clusters and (3, 3), (4, 4), (5, 3), and (5, 5) chiral SWAuTs[9] are involved. In the case of carbon (Figure 3a), it is noted that the E_b of the 1 ML

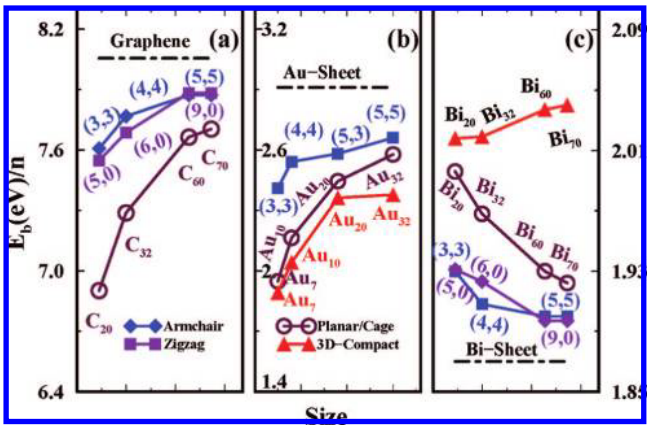

Figure 3. Comparisons of the E_b of a monolayer sheet, cage, and 3D X_n (X = C, Au, and Bi) structures and the corresponding infinite tubes with similar pore diameters: (a) carbon, (b) gold, and (c) bismuth. In (a) and (c): $n = 20$, 32, 60, and 70; in (b): $n = 7$, 10, 20, and 32.

graphite (graphene) is about 8.054 eV, which is higher than those of the CNTs, from 7.607 (7.546) eV for the (3, 3) ((5, 0)), 7.767 (7.871) eV for the (4, 4) ((6, 0)), to 7.871 (7.882) eV for the (5, 5) ((9, 0)) tube, respectively. The E_b of the carbon cages increases monotonously from 6.901 eV (C_{20}), 7.287 eV (C_{32}), to 7.664 eV (C_{60}). Our calculations show that the 3D C_n are far less stable than the cages. In fact, if we manually squash some surface atoms inside the cages, the collapsed structure can be readily optimized back to cages. Importantly, the binding energies of these cages are systematically lower than those of the corresponding tubes, which are lower again than that of the planar graphene.

A similar phenomenon is observed for gold. The average binding energies of the planar or cagelike Au_n ($n = 7$, 10, 20, and 32) are clearly greater than those of their 3D compact isomers due to the enhanced s−d hybridizations induced by the relativistic effects, in close agreement with previously reported results.[6] Interestingly, the average binding energies of the 2D-like and 3D-compact (D_{5h}-Au_7, T_d-Au_{10}, C_{2v}-Au_{20}, and amorphous-Au_{32}) clusters are lower than that of the chiral single-wall gold tubes,[9] which are again lower than that of the Au(111) sheet. We note that the recent investigations on the boron system also show such a trend: the binding energies of the SWBNTs are less than that of the boron sheet.[4] All the above results seem to support a general conclusion that the relative stabilities of the structures are E_b(3D) < E_b(2D-cage) < E_b(2D-sWNT) < E_b(2D-sheet), or the nanocages are always less stable than the nanotubes, if the latter are stable.

This conclusion may be explained from the bonding characteristics and the curvature effect. For elements that can form a planar structure, the atomic bonding show strongly planar electronic distribution, e.g., in sp^2 and sd^n hybridization in carbon and gold, respectively. When such a structure is curved from the planar configuration, the binding energy (stability) is lowered due to curvature. Because of the quantum size effect, the enlarged energy gaps between different electronic orbitals (bands) at the meso- or nanoscale may reduce the tendency for new hybridization, such as the 3D sp^3-like bonding in a nanodiamond structure.[20] Consequently, the planner bonding, e.g., in sp^2-like carbon, is the determining factor for the stability of a quasi-planar structure. Curvature may play a key role in the relative stabilities of the different quasi-2D nanostructures. As reported in ref 21, the curvature energy (per atom) of a (n, n) CNT or a spherical fullerene with N atoms can be written in the form $E_{CNT} \approx \epsilon'(d/r)^2 = \epsilon_1/n^2$ or $E_{CNC} \approx \epsilon''(d/r)^2 = \epsilon_2/N$, respectively. Here the magnitude of parameter ϵ' or ϵ'' may

depend very slightly on the chirality of the tube or the size of the fullerene cage. The curvature is proportional to the ratio of the C−C bond length d over the tube (fullerene cage) radius r, i.e., d/r. The overall curvature effect (energy) is lower in a CNT than in a CNC of a similar diameter. Hence, the CNT is more stable than the CNC.

However, the opposite trend of the relative stabilities seems true for the Bi nanostructures, as shown in Figure 3c. The calculated E_b is about 1.874 eV for the optimized Bi sheet, which is clearly smaller than those of the SWBiNTs, from 1.930 (1.931) to 1.900 (1.897) eV as the tube size increases from (3, 3) ((5, 0)) to (5, 5) ((9, 0)). Further comparison shows that both the cagelike and 3D Bi_n (n = 20, 32, 60, 70) possess higher binding energies than the corresponding SWNTs (Figure 3b); i.e., the latter are even more stable than the former. From the energy curve (Figure 3c), the E_b of the 3D structure increases with the cluster size, which is a general trend for most elements, indicating that the currently obtained stable structures are in the ground states or low-lying states. The above results for Bi indicate that if the NCs are unstable, the NTs will be even less stable, as observed in semimetal element bismuth. In this case, the relative stabilities of different nanostructures are E_b(3D) > E_b(2D-cage) > E_b(2D-tube) > E_b(2D-sheet).

Similarly, the above observation can also be explained by the atomic bonding and the curvature effect. For a given element, if its intrinsic bonding favors a 3D structure, energy must be consumed to confine the out-of-plane bonds into the planar structures. For example, because of the weak s^xp^3-like ($x \approx 0.1$) bonding in bismuth,[19] to form a planar or a quasi-planar cage or a tube structure, at least one p-bond will be largely distorted for each Bi atom, which dramatically reduces its stability, particularly in the larger 2D structures with smaller curvatures. This is also the reason why a relatively high activity is observed in the flat regions of the Bi_{32} cage.

It is also noted that both thermodynamic and kinetic properties contribute to the stability of a structure. In the cases of carbon and gold, large activation barriers may exist for transformation between different phases, such as cages, tubes, graphite, and diamond, as these phases are sufficiently stable, and there are large energy differences between these structures (Figures 3a,b). Thus, various metastable structures can be sustained. In contrast, only very small energy differences are detected in the different phases of bismuth, and hence small activation energies are needed to break the weak Bi−Bi bonds and induce phase changes to a relatively stable structure, e.g., from 2D-NTs to 3D-NWs.[13] In practice, other factors such as temperature, catalysts, strain, and chirality may also affect the stabilities of the nanostructures,[21,22] which is beyond the scope of this investigation.

IV. Summary

To summarize, we have identified the relative stabilities of several types of nanostructures. There is a strong relationship between the stabilities of a nanocage and a nanotubes for a given element. If the intrinsic structure of an element favors a planar configuration, such as the layered structure of semiconductive carbon, boron and fcc Au(111) layered metal gold, the relative stability (binding energy per atom) of the nanostructures seems to vary in the following order: E_b(3D) < E_b(2D-cage) < E_b(2D-tube) < E_b(2D-sheet). The variation is due to the tailored bonding characteristics by the curvature effect. In this case, their NTs can be constructed upon the existence of a NC precursor. On the other hand, for an element that favors a densely packed structure, the stability sequence thoroughly reverses: E_b(3D) > E_b(2D-cage) > E_b(2D-tube) > E_b(2D-sheet). The confirmed example here is semimetal bismuth, where the energetically favorable nanostructures for different scales should be 3D-like. Therefore, an inference from the above is the following: If a NC is (not) stable, then its SWNT is even more (less) stable; i.e., no cage, no tube. (The only exception is the limiting case: when the 2D cage and 3D structures degenerate and the cage is slightly unstable, the nanotube may still be stable if its binding energy is far higher than the cage.) The above findings are important in continued exploration of two-dimensional nanostructures and in the design and assembly of nanodevices.

Acknowledgment. The authors gratefully acknowledge the support by the National Science Foundation of China under Grant 10604049 and the UK EPSRC under UK-SHEC(EP/E040071/1), a Platform Grant (EP/E046193/1), and EP/F013612/1.

References and Notes

(1) (a) Kroto, H. W.; Heath, J. R.; O'Brien, S. C.; Curl, R. F.; Smalley, R. E. *Nature (London)* **1985**, *318*, 162. (b) Hedberg, K.; Hedberg, L.; Bethune, D. S.; Brown, C. A.; Dorn, H. C.; Johnson, R. D.; De Vries, M. *Science* **1991**, *254*, 410.

(2) Iijima, S. *Nature (London)* **1991**, *354*, 56.

(3) Geim, A. K.; Novoselov, K. S. *Nat. Mater.* **2007**, *6*, 183, and references therein.

(4) Szwacki, N. G.; Sadrzadeh, A.; Yakobson, B. I. *Phys. Rev. Lett.* **2007**, *98*, 166804.

(5) (a) Oku, T.; Nishiwaki, A.; Narita, I.; Gonda, M. *Chem. Phys. Lett.* **2003**, *380*, 620. (b) Zope, R. R.; Baruah, T.; Pederson, M. R.; Dunlap, B. I. *Chem. Phys. Lett.* **2004**, *393*, 300, and references therein.

(6) (a) Gu, X.; Ji, M.; Wei, S. H.; Gong, X. G. *Phys. Rev. B* **2004**, *70*, 205401. (b) Johansson, M. P.; Sundholm, D.; Vaara, J. *Angew. Chem., Int. Ed.* **2004**, *43*, 2678. (c) Bulusu, S.; Li, X.; Wang, L. S.; Zeng, X. C. *Proc. Natl. Acad. Sci. U.S.A.* **2006**, *103*, 8326, and references therein.

(7) (a) Tang, H.; Ismail-Beigi, S. *Phys. Rev. Lett.* **2007**, *99*, 115501. (b) Singh, A. K.; Sadrzadeh, A.; Yakobson, B. I. *Nano Lett.* **2008**, *8*, 1314. (c) Kiran, B.; Bulusu, S.; Zhai, H.-J.; Yoo, S.; Zeng, X. C.; Wang, L. S. *Proc. Natl. Acad. Sci. U.S.A.* **2005**, *102*, 961, and references therein.

(8) (a) Chopra, N. G.; Luyken, R. J.; Cherrey, K.; Crespi, V. H.; Cohen, M. L.; Louie, S. G.; Zettl, A. *Science* **1995**, *269*, 966. (b) Mickelson, W.; Aloni, S.; Han, W.-Q.; Cumings, J.; Zettl, A. *Science* **2003**, *300*, 467.

(9) (a) Senger, R. T.; Dag, S.; Ciraci, S. *Phys. Rev. Lett.* **2004**, *93*, 196807. (b) Oshima, Y.; Onga, K.; Takayanagi, A. *Phys. Rev. Lett.* **2003**, *91*, 205503.

(10) Hofmann, Ph. *Prog. Surf. Sci.* **2006**, *81*, 191.

(11) (a) Tian, Y.; Meng, G.; Biswas, S. K.; Ajayan, P. M.; Sun, S.; Zhang, L. *Appl. Phys. Lett.* **2004**, *85*, 967. (b) Heremans, J.; Thrush, C. M.; Lin, Y.-M.; Cronin, S.; Zhang, Z.; Dresselhaus, M. S.; Mansfield, J. F. *Phys. Rev. B* **2000**, *61*, 2921. (c) Heremans, J.; Thrush, C. M.; Zhang, Z.; Sun, X.; Dresselhaus, M. S.; Ying, J. Y.; Morelli, D. T. *Phys. Rev. B* **1998**, *58*, 10091(R)

(12) (a) Liu, K.; Chien, C. L.; Searson, P. C.; Yu-Zhang, K. *Appl. Phys. Lett.* **1998**, *73*, 1436. (b) Zhang, Z. B.; Ying, J. Y.; Dresselhaus, M. S. *J. Mater. Res.* **1998**, *13*, 1745.

(13) Li, Y.; Wang, J.; Deng, Z.; Wu, Y.; Sun, X.; Yu, D.; Yang, P. *J. Am. Chem. Soc.* **2001**, *123*, 9904.

(14) (a) Kohn, W.; Sham, L. J. *Phys. Rev.* **1965**, *140*, A1133. (b) Schlter, M.; Sham, L. J. *Phys. Today* **1982**, *35*, 36.

(15) (a) Perdew, J. P.; Wang, Y. *Phys. Rev. B* **1992**, *45*, 13244. (b) Perdew, J. P.; Chevary, J. A.; Vosko, S. H.; Jackson, K. A.; Pederson, M. R.; Singh, D. J.; Fiolhais, C. *Phys. Rev. B* **1992**, *46*, 6671.

(16) (a) Kresse, G.; Furthmller, J. *Phys. Rev. B* **1996**, *54*, 11169. (b) *Comput. Mater. Sci.* **1996**, *6*, 15.

(17) (a) Blöchl, P. E. *Phys. Rev. B* **1994**, *50*, 17953. (b) Kresse, G.; Joubert, D. *Phys. Rev. B* **1999**, *59*, 1758.

(18) Monkhorst, H. J.; Pack, J. D. *Phys. Rev. B* **1976**, *13*, 5188.

(19) Gao, L.; Li, P.; Lu, H.; Li, S. F.; Guo, Z. X. *J. Chem. Phys.* **2008**, *128*, 194304.

(20) Lee, G.-D.; Wang, C. Z.; Yu, J.; Yoon, E.; Ho, K. M. *Phys. Rev. Lett.* **2003**, *91*, 265701.

(21) (a) Adams, G. B.; Sankey, O. F.; Page, J. B.; O'Keeffe, M.; Drbold, D. A. *Science* **1992**, *256*, 1792. (b) Park, N.; Lee, K.; Han, S.; Yu, J.; Ihm, J. *Phys. Rev. B* **2002**, *65*, 121405(R)

(22) Bandow, S.; Asaka, S.; Saito, Y.; Rao, A. M.; Grigorian, L.; Richter, E.; Eklund, P. C. *Phys. Rev. Lett.* **1998**, *80*, 3779.

JP8052289